



OPEN

Comparisons in temperature and photoperiodic-dependent diapause induction between domestic and wild mulberry silkworms

Takeshi Yokoyama^{1,8}, Shigeru Saito^{2,8}, Misato Shimoda³, Masakazu Kobayashi⁴, Yoko Takasu⁵, Hideki Sezutsu⁵, Yoshiomi Kato⁶, Makoto Tominaga², Akira Mizoguchi⁷ & Kunihiro Shiomi⁴✉

The bivoltine strain of the domestic silkworm, *Bombyx mori*, has two generations per year. It shows a facultative diapause phenotype determined by environmental conditions, including photoperiod and temperature, and nutrient conditions during embryonic and larval development of the mother. However, it remains unclear how the environmental signals received during development are selectively utilized as cues to determine alternative diapause phenotypes. We performed a comparative analysis between the Kosetsu strain of *B. mori* and a Japanese population of the wild mulberry silkworm *B. mandarina* concerning the hierarchical molecular mechanisms in diapause induction. Our results showed that for the Kosetsu, temperature signals during the mother's embryonic development predominantly affected diapause determination through the thermosensitive transient receptor potential ankyrin 1 (TRPA1) and diapause hormone (DH) signaling pathways. However, embryonic diapause in *B. mandarina* was photoperiod-dependent, although the DH signaling pathway and thermal sensitivity of TRPA1 were conserved within both species. Based on these findings, we hypothesize that TRPA1-activated signals are strongly linked to the signaling pathway participating in diapause induction in Kosetsu to selectively utilize the temperature information as the cue because temperature-dependent induction was replaced by photoperiodic induction in the TRPA1 knockout mutant.

In the domestic silkworm *Bombyx mori*, progeny diapause is induced during the early embryonic stage. The development of diapause-destined embryos is arrested during the G2 cell cycle stage immediately after forming the cephalic lobe and telson and sequential segmentation of the mesoderm and ectoderm¹. In bivoltine strains, populations of *B. mori* that have two generations per year show a facultative diapause phenotype, which is determined by environmental conditions, such as photoperiod, temperature, and nutrient conditions during embryonic and larval development in the mother's generation². In general, progeny diapause of bivoltine strains is predominantly determined by environmental conditions during maternal embryonic development in conjunction with long days and high temperatures that induce diapause eggs²⁻⁴. However, the environmental cues that induce diapause are different in each bivoltine strain and are also updated by integrating cumulative signals received through development^{5,6}. For instance, when larvae were reared on an artificial diet under long-day conditions, some silkworm strains produced non-diapause eggs even if the eggs were incubated in diapause

¹Department of United Graduate School of Agricultural Science, Tokyo University of Agriculture and Technology, Fuchu 183-8509, Japan. ²Division of Cell Signaling, National Institute for Physiological Sciences, National Institutes of Natural Sciences, Okazaki, Japan. ³Gunma Sericultural Technology Center, Maebashi 371-0852, Japan. ⁴Faculty of Textile Science and Technology, Shinshu University, Ueda, Nagano 386-8567, Japan. ⁵National Institute of Agrobiological Sciences (NIAS), Tsukuba 305-8602, Japan. ⁶International Christian University, Mitaka 181-8585, Japan. ⁷Division of Liberal Arts and Sciences, Aichi Gakuin University, Nisshin 470-0195, Japan. ⁸These authors contributed equally: Takeshi Yokoyama and Shigeru Saito ✉email: shiomi@shinshu-u.ac.jp

egg-producing conditions^{2,7}. However, it remains unclear how environmental signals received through development are selectively utilized as cues to determine alternative diapause phenotypes.

For the bivoltine strain Kosetsu, the temperature signal during the mother's embryonic development is the predominant factor affecting diapause determination, regardless of the photoperiods during embryonic and larval development under our rearing condition using an artificial diet^{8,9}. When incubating eggs at 25 °C under continuous darkness (25DD), the resultant female moths lay nearly 100% diapause eggs. In contrast, incubation of eggs at 15 °C in dark conditions (15DD) resulted in moths that lay nearly 100% non-diapause eggs. Thus, Kosetsu is considered a typical strain that is susceptible to temperature-dependent diapause induction.

The molecular mechanisms underlying the induction of *B. mori* embryonic diapause have been investigated extensively^{5,9}. Our previous study revealed that embryonic diapause is induced by the diapause hormone (DH) signaling pathway, consisting of a highly sensitive and specific interaction between DH and DH receptors (DHR) pupal-adult development⁸. *DH-PBAN* encodes a polyprotein precursor containing DH, pheromone biosynthesis activating neuropeptide (PBAN), and α -, β -, and γ -subesophageal ganglion (SG) neuropeptides (SGNPs). DH is produced from the DH-PBAN precursor through posttranslational processing¹⁰. It is produced exclusively in seven pairs of neurosecretory cells, known as DH-PBAN-producing neurosecretory cells (DHPCs), located within the SG in the mother's generation¹¹. DH is released from the corpus cardiacum (CC)¹², a major release site for neuropeptide hormones, into the hemolymph, and acts on DHR in ovary¹³. Furthermore, the cerebral γ -aminobutyric acid (GABA)ergic and corazonin (Crz) pathway modulates DH release throughout the temperature-dependent expression of the plasma membrane GABA transporter⁹. Recent studies revealed that the transient receptor potential ankyrin 1 (TRPA1) (*BmoTRPA1*) acts as a thermosensitive channel activated at temperatures above ~21 °C and affects diapause induction through DH release in Kosetsu. Thus, *BmoTRPA1* acts as a molecular switch for the temperature-dependent diapause induction in Kosetsu¹⁴.

B. mori was domesticated from the wild mulberry silkworm, *B. mandarina*, approximately 5000–10,000 years ago in China^{15–18}. *B. mori* and *B. mandarina* are similar in morphological, cytological, and physiological aspects; copulation between them is possible, and the resultant progeny is never sterile^{19–21}, although both species are clearly genetically differentiated²². In addition, *B. mandarina* enters embryonic diapause at a similar developmental stage as in *B. mori*^{23,24}. The bi-, tri-, and univoltine *B. mandarina* inhabit Japan based on the moth's seasonal fluctuation^{25,26}. Furthermore, photoperiodic-dependent diapause induction of *B. mandarina* was shown in a previous report, in which more female moths produced diapause eggs under short-day conditions, such as a 12-h light/12-h dark cycle (12L12D) than under long-day conditions, such as 15L9D during larval stages, even if the temperature was kept constant at 25 °C during embryonic development. Diapause induction is most strongly affected by photoperiod in a certain developmental stage following the second larval ecdysis²⁷. Thus, to our knowledge, *B. mandarina* enters diapause by photoperiodic induction, which contrasts with the temperature-dependent diapause induction in Kosetsu of *B. mori*. Therefore, we performed a comparative analysis of diapause induction using Kosetsu and a Japanese population of *B. mandarina* with respect to the hierarchical molecular mechanisms to elucidate the selectivity and integration of environmental cues. In the present study, we hypothesize that TRPA1-mediated signals are strongly linked to the signaling pathway participating in diapause induction in Kosetsu to selectively utilize the temperature information as the cue.

Results and discussion

Temperature and photoperiodic-dependent diapause induction are different between the Kosetsu strain of *B. mori* and the Fuchu population of *B. mandarina*. We first confirmed the photoperiodic response in diapause induction of *B. mandarina* as described previously²⁷. When eggs were incubated under 25DD during embryonic development, and thereafter, the larvae reared under long-day conditions, 16L8D and 24L0D, eclosed moth laid non-diapause eggs that hatched 10 d after oviposition (Fig. 1a,b). In contrast, most eggs were pigmented and never hatched 30 d after oviposition under short-day condition, 8L16D, for 25DD embryos. These pigmented eggs arrested normal embryogenesis, and the arrested stage was similar to that in diapause eggs in *B. mori* (Fig. 1a,c). The progeny eggs entered diapause under all photoperiodic conditions when embryos were reared under 25DD in *B. mori* (Fig. 1b), indicating that there were differences in the environmental cues also temperature or photoperiodic-dependent diapause induction in both strains. However, both strains never entered diapause for progeny from the 15DD condition (Fig. 1b).

DH induces progeny diapause in *B. mandarina*. To clarify whether the DH signaling pathway is involved in diapause induction in *B. mandarina*, we determined the complementary DNA (cDNA) sequences of *DH-PBAN* and *DHR*. The *B. mandarina* *DH-PBAN* cDNA was cloned, and the deduced amino acid sequence of DH (*BmaDH*) was identical to that of *B. mori* DH (*BmoDH*)²⁸ (Supplementary Fig. S1). We also found the homologous sequence to *B. mori* *DHR* (*BmoDHR*) cDNA using SilkBase (<http://silkbases.ab.a.u-tokyo.ac.jp/cgi-bin/index.cgi>). Using reverse transcription PCR (RT-PCR), we cloned *B. mandarina* *DHR* cDNA (*BmaDHR*; Acc. No. LC594680). The sequence of the deduced amino acids in *BmaDHR* represented a highly similar sequence in *BmoDHR* at 97%, including the seven transmembrane regions (TM1–TM7) (Supplementary Fig. S1). Next, immunostaining was performed using an anti-DH antibody. High-immunofluorescent signals were detected as a cluster of somata in SG (Fig. 2a,c), considering that these immunoreactive clusters of somata were identical to SMd, SMx, SLb, and SL neurons of DHPCs in *B. mori*¹² (Fig. 2b,c). Furthermore, immunoreactive neurites with bead-like varicosities were detected in the CC and projected onto the corpus allatum (CA) surface to form blind ends like that of *B. mori* (Fig. 2d), suggesting that *BmaDH* was released to the hemolymph through these neurohemal organs.

Next, we injected synthetic DH into *B. mandarina* pupae developed from 25 and 15DD embryos and reared under the 16L8D condition (Fig. 2e). Although peanut oil-injected silkworms never oviposited diapause eggs,

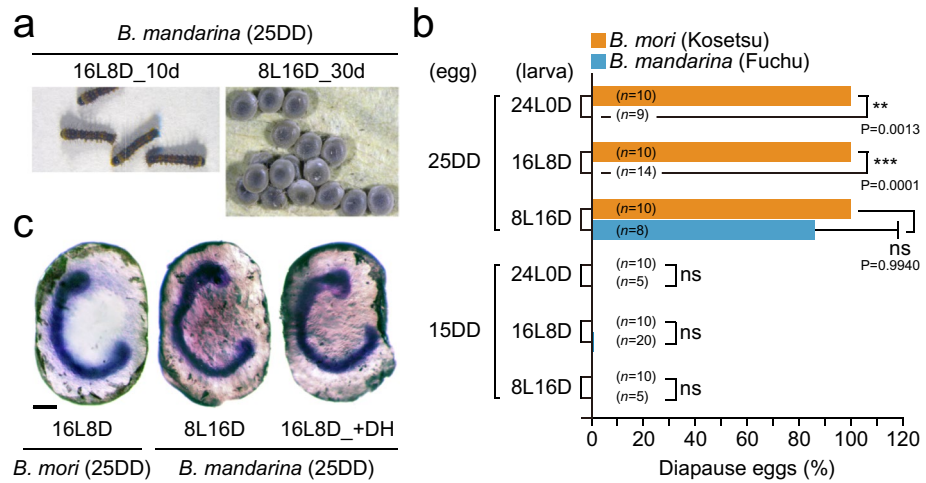


Figure 1. Temperature and photoperiodic diapause induction in *Bombyx mori* and *B. mandarina*. (a) The typical larvae and eggs of the wild mulberry silkworm *B. mandarina*. Eggs were incubated at 25DD; after that, larvae were reared at 16L8D or 8L16D. Progeny eggs hatched on 10 d after oviposition under the 16L8D condition, whereas progeny eggs never hatched by 30 d after oviposition under the 8L16D condition. (b) Effects of temperature and photoperiodic conditions during embryonic and larval stages on diapause egg-inducing activity in the Kosetsu strain of *B. mori* and a Fuchu population of *B. mandarina*. After eggs were incubated under the 25DD or 15DD condition, larvae were reared on 24L0, 16L8D, and 8L16D conditions. Each bar represents the mean \pm SD of 5–20 animals. Significant differences represented in *B. mori* versus *B. mandarina* are in the same condition. ns, non-significant; **, $P < 0.01$; ***, $P < 0.001$. (c) Thionin staining of embryos 30 d after oviposition of domestic silkworm *B. mori* in 16L8D (25DD), and 30 d after oviposition of *B. mandarina* in both 8L16D and DH-injected silkworm in 16L8D (25DD). Scale bar = 200 μ m.

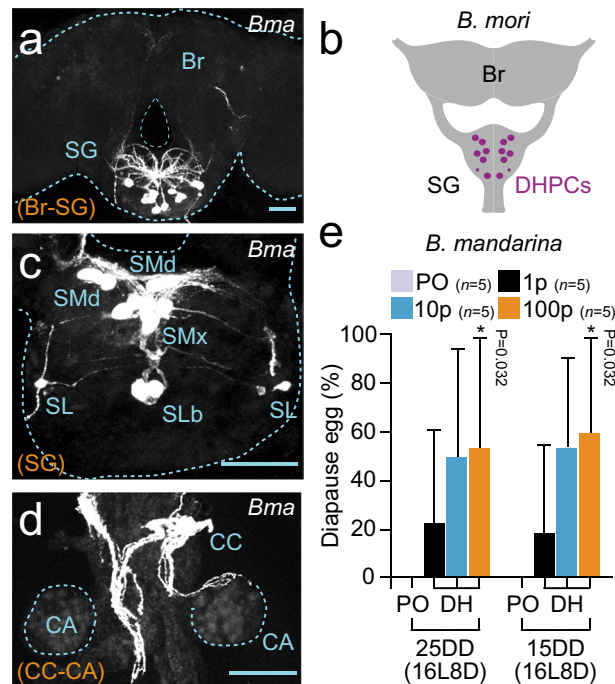


Figure 2. Diapause hormone (DH) induces egg diapause in *B. mandarina*. (a, c, d) Immunostaining of anti-DH[N] antibody in brain-subesophageal ganglion (SG) complex (a), SG (c), and corpus allatum (CA)–corpus cardiacum (CC) complex (d) of *B. mandarina* pupa. Tissues were dissected out on 1 d after pupation from 8L16D (25DD) pupae. Scale bar = 100 μ m. (b) Schematic drawing of pupal brain–SG complex in *Bombyx mori*. DH is produced in DH-PBAN-producing neurosecretory cells (DHPCs) located within the SG. (e) Diapause egg-inducing activity of DH injection. Peanut oil (PO) or each DH peptide concentration (1, 10, or 100 pmol) was injected into *B. mandarina* pupa reared under the 16L8D condition from 25 and 15DD embryos, and diapause egg-inducing activity was measured. Each bar represents the mean \pm SD of five animals. Asterisks indicate significant differences versus PO injection. *, $P < 0.05$.

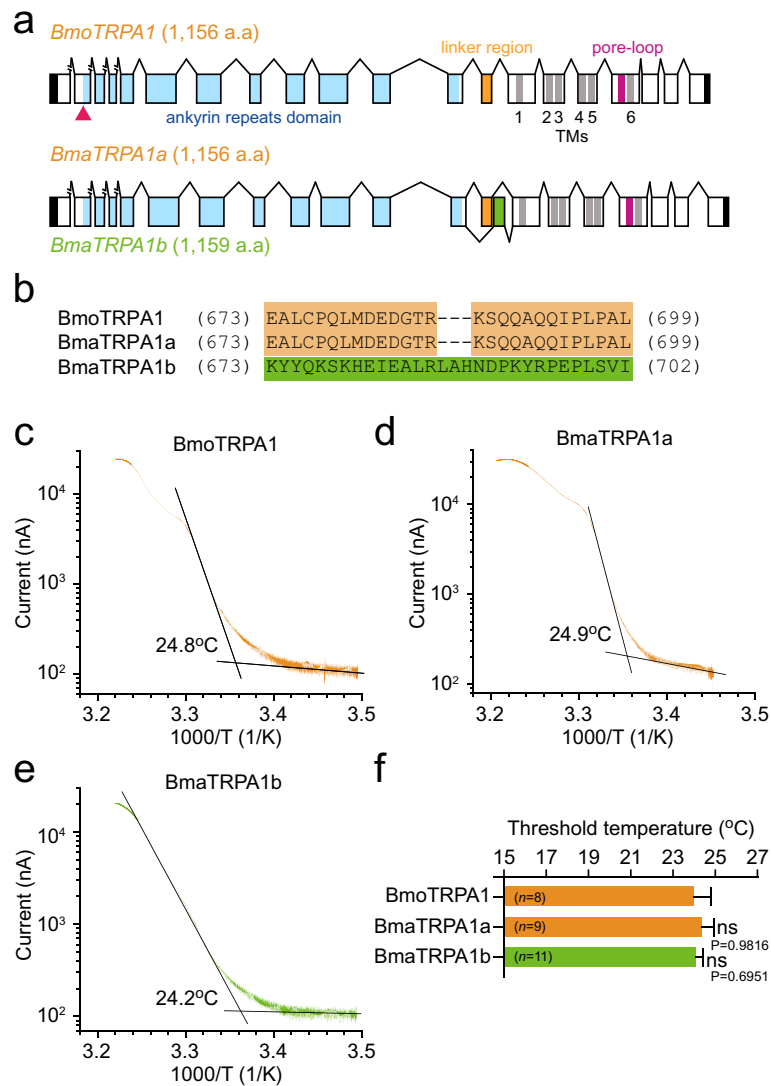


Figure 3. Cloning and functional analysis of *Bombyx mori* and *B. mandarina* TRPA1. **(a)** Schematic representations of the *B. mori* TRPA1 (*BmoTRPA1*), *B. mandarina* TRPA1a (*BmaTRPA1a*), and TRPA1b (*BmaTRPA1b*). Boxes and lines represent exons and introns, respectively. Black, blue, orange, gray, and red boxes represent domains of untranslated regions, ankyrin repeat, linker region, transmembrane (1–6), and pore-loop, respectively. The red triangle indicates the TALEN target site. **(b)** Sequence alignment of the linker region between TRPA1s. **(c–e)** Arrhenius plots for the heat-induced *BmoTRPA1*, *BmaTRPA1a*, and *BmaTRPA1b* current shows a clear flex point in temperature dependency. Each temperature threshold for TRPA1 activation was defined as when the two linear-fitted lines crossed (i.e., a flex point). **(f)** Comparison of threshold temperature for each TRPA1. Each bar represents the mean \pm SEM of 8–11 samples. Significant differences versus *BmoTRPA1* were evaluated. ns, non-significant.

DH-injected silkworms oviposited diapause eggs in a dose-dependent manner. The diapause eggs were staged in the early embryonic stages, which was similar to the cases of diapause eggs of *B. mandarina* (8L16D) and *B. mori* (Fig. 1c, 16L8D + DH). Therefore, we concluded that the DH signaling pathway is conserved between *B. mori* and *B. mandarina* to induce progeny diapause.

Cloning and functional analysis of TRPA1 orthologs in *B. mandarina*. We cloned two TRPA1 cDNAs, namely *BmaTRPA1a* (Acc. No. LC597009.1) and *BmaTRPA1b* (Acc. No. LC597010.1), from *B. mandarina* eggs just before hatching. The amino acid sequences deduced from the two cDNAs (*BmaTRPA1a* and *BmaTRPA1b*) were highly similar to that of *BmoTRPA1* at 99% and 97%, respectively (Fig. 3a and Supplementary Fig. S2). The *BmaTRPA1* genes are conserved in the functional domain consisting of ankyrin repeat domains (ANK1–17), transmembrane domains (TM1–6), and a pore-loop domain among the TRPA1 subfamily^{29,30}. *BmaTRPA1a* and *BmaTRPA1b* transcripts were caused by alternative splicing of distinct exons encoding the linker region located between the last ankyrin repeat and the first transmembrane segment (Fig. 3a,b, and Sup-

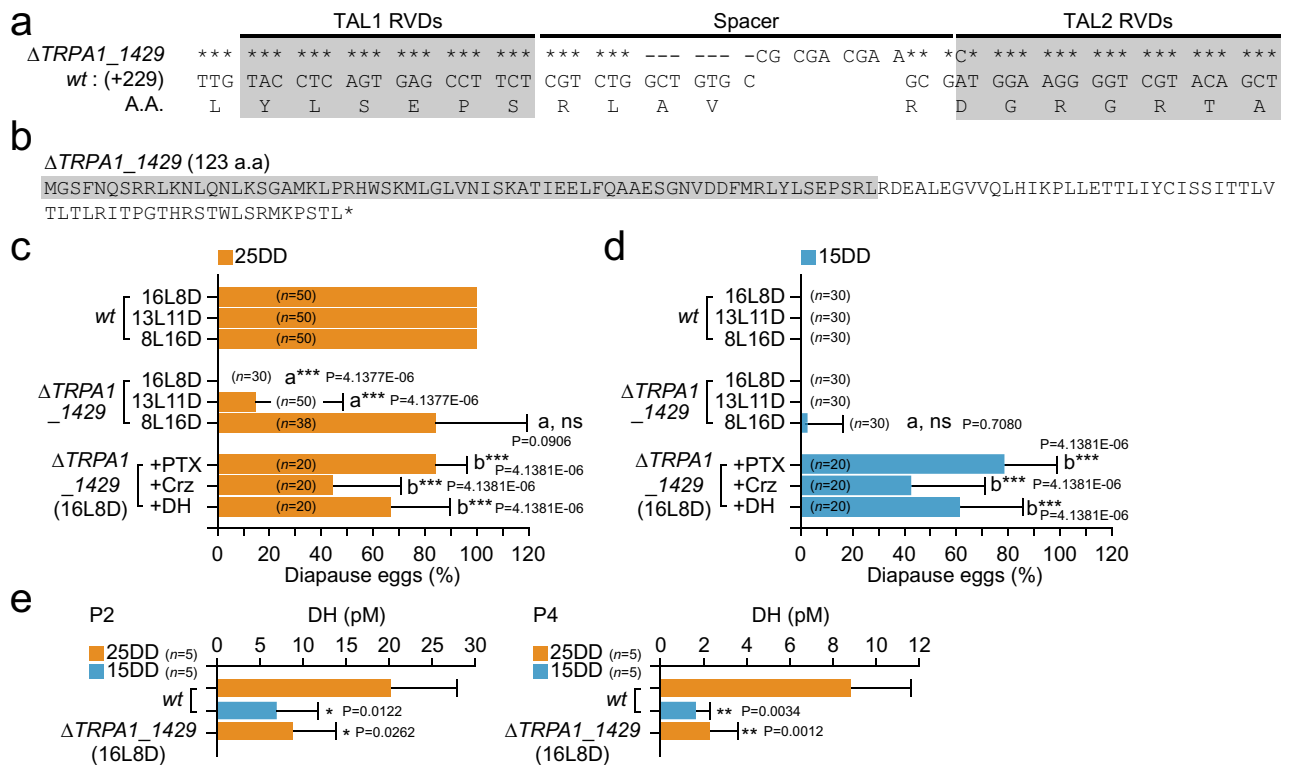


Figure 4. Knockout (KO) mutant of *BmoTRPA1*. (a) Gray boxes indicate the sequences of the TALEN target sites. The sequence of the *BmoTRPA1* gene of the mutant line $\Delta TRPA1_{1429}$ that inserted, deleted, and replaced 17 bases between the spacer region and right TALEN binding site (TAL2 RVDs) are indicated. Asterisks indicate the bases identical to wild type (*wt*) sequences. (b) The $\Delta TRPA1_{1429}$ gene encodes a truncated protein consisting of 123 amino acids. (c, d) Diapause egg-inducing activity in $\Delta TRPA1_{1429}$. The proportions of diapause eggs oviposited from *wt* and KO mutant female moths of 25DD (c) and 15DD (d) were measured as well as that of moths injected with plant alkaloid picrotoxin (PTX), corazonin (Crz), and diapausing hormone (DH) at 50 μ g, 1 nmol, and 100 pmol/pupa, respectively. Significant differences versus *wt* (a) or non-injected silkworm on 16L8D (b) were evaluated. (e) DH levels in hemolymph 2 (P2) and 4 (P4) d after pupation in both *wt* and $\Delta TRPA1_{1429}$. Significant differences versus *wt* (25DD) were evaluated. ns, non-significant; *, $P < 0.05$; **, $P < 0.01$; ***, $P < 0.001$.

plementary Fig. S2). This structure resembles the alternative splicing variants of TRPA1 found in *Drosophila melanogaster* and *Aedes aegypti*^{29,30}.

Next, channel properties of TRPA1 between the two species were compared by an electrophysiological approach. BmaTRPA1 or BmoTRPA1 were heterologously expressed in *Xenopus* oocytes, and ionic currents were observed. TRPA1 from both species was activated by heat. We investigated temperature sensitivity and determined the threshold temperature for activation for BmaTRPA1a and BmaTRPA1b as well as BmoTRPA1 with an Arrhenius plot (Fig. 3c–f). The average thermal activation threshold of BmoTRPA1 was $24.0\text{ }^{\circ}\text{C} \pm 0.8\text{ }^{\circ}\text{C}$ (Fig. 3c). This value is slightly higher than that of BmoTRPA1 previously reported using mammalian cultured cells (approximately $21\text{ }^{\circ}\text{C}$)¹⁴, which might be caused by different cell types used for heterologous expression of TRPA1. The average thermal activation thresholds of BmaTRPA1a and BmaTRPA1b were $24.4\text{ }^{\circ}\text{C} \pm 0.6\text{ }^{\circ}\text{C}$ and $24.0\text{ }^{\circ}\text{C} \pm 0.4\text{ }^{\circ}\text{C}$, respectively. No statistical difference was observed among thermal activation thresholds for BmoTRPA1, BmaTRPA1a, and BmaTRPA1b (Fig. 3f). Therefore, we concluded that the embryonic expression and temperature sensitivity of TRPA1 are conserved in both species.

Knockout (KO) analysis of BmoTRPA1 in diapause induction. Since both temperature-sensitive TRPA1 and DH signaling pathways are conserved in *B. mori* and *B. mandarina*, we hypothesized that there were differences in the downstream signal of TRPA1 activation to induce diapause between *B. mori* and *B. mandarina*. Hence, we constructed a KO mutant of *BmoTRPA1* to investigate the TRPA1-activated downstream pathway. We designed a transcription activator-like effector nuclease (TALEN) target in the second exon encoding the first ankyrin repeat (ANK1) (Figs. 3a, 4a, and Supplementary Fig. S2). We isolated a homozygous mutant in which both a 7-base sequence was deleted, and a 9-base sequence was inserted into the spacer region between two TALEN binding sites, and a single base pair was replaced in the right TALEN binding site (TAL2) and designated the mutant as $\Delta TRPA1_{1429}$ (Fig. 4a,b). $\Delta TRPA1_{1429}$ was considered a null mutant, which could not translate full-length *BmoTRPA1* due to a frameshift of *BmoTRPA1* cDNA. We then investigated whether the $\Delta TRPA1_{1429}$ silkworm oviposited non-diapause eggs from 25 and 15DD (Fig. 4c,d). Although the wild type (*wt*) moths laid 100% of diapause eggs, all $\Delta TRPA1_{1429}$ moths laid only non-diapause eggs when the

larvae were reared under the long-day condition (16L8D). In this condition, the hemolymph DH levels of $\Delta TRPA1_{1429}$ from 25DD embryos were extremely low compared with those of *wt* for both samples collected 2 and 4 days after pupation, resulting in decreased levels similar to the 15DD of *wt* (Fig. 4e). Furthermore, when picrotoxin (PTX), Crz, or DH were injected into $\Delta TRPA1_{1429}$ pupa under the 16L8D condition, higher diapause egg-inducing activity was observed, suggesting that the GABAergic, Crz, and DH signaling pathways were retained in $\Delta TRPA1_{1429}$ as those in 15DD silkworms (Fig. 4d).

However, the ratios of non-diapause eggs gradually decreased depending on the length of scotophase in $\Delta TRPA1_{1429}$. The percentages of diapause eggs were 14.7% and 84.6% in 13L11D and 8L16D, respectively (Fig. 4c). Taken together, we speculated that the BmoTRPA1-activated pathway is involved in diapause induction in the *wt* of Kosetsu through the GABAergic, Crz, and DH signaling pathways, because the disruption of the TRPA1-activated pathway in the BmoTRPA1 KO mutant could not operate the temperature-dependent diapause induction. Interestingly, BmoTRPA1 KO mutants' progeny eggs exhibited photoperiodic diapause induction, as is the case with *B. mandarina*. This suggests that the *wt* of Kosetsu potentially possesses a signaling pathway involved in photoperiodic diapause induction that might be canceled by the strong linkage of the BmTRPA1-activated signal and DH signaling pathways. Consequently, the progeny diapause may be dependent on photo- or scotophase-length in BmoTRPA1 KO mutants such as *B. mandarina*. To our knowledge, the temperature-dependent diapause induction did not occur in *B. mandarina*. Therefore, we propose that the temperature-dependent diapause induction phenotype was artificially selected and spread throughout *B. mori* populations during the ancient domestication process, given the fact that temperature regulation was much easier than photoperiodic control by humans. Moreover, both *B. mandarina* and the TRPA1 mutant of *B. mori* only entered diapause under short-day conditions at 25 °C but could not do so at 15 °C. Therefore, BmTRPA1 might play a partial role in signaling, and other unidentified additional factors (e.g., cold-sensitive thermosensors activated at ≤ 15 °C) may also be involved in diapause induction. Furthermore, as it is suggested that insect clocks are engaged in photoperiodic response, including diapause induction³¹, both the temperature and photoperiodic diapause induction may be mediated by common unidentified machinery such as circadian clocks. In this study, we investigated to elucidate the molecular mechanism of selectivity and integration of environmental cues concerning diapause induction. Our results demonstrated the usefulness of a comparative study using the Kosetsu strain of *B. mori* and a Japanese population of *B. mandarina* for further research on diapause induction.

Methods

Silkworms. For *B. mori*, the bivoltine Kosetsu strain was used in these experiments. Eggs were incubated under two different conditions: (1) at 25 °C under continuous darkness (25DD) to obtain diapause eggs in the *wt*, and (2) at 15 °C under continuous darkness (15DD) to obtain non-diapause eggs. Larvae were then reared on an artificial diet (Kuwano-hana for young silkworm, Gunma Artificial Diet Production Center, Takasaki, Gunma) at 25 °C–27 °C under 16-h light/8-h dark (16L8D), 13L11D, 8L16D, and 24L0D cycles at a relative humidity of 30–50%. Pupae used in the experiments were collected within 1 h after each ecdysis (referred to as day 0) to synchronize their subsequent development. Pupae were incubated at 25 °C to allow for adult development. The larvae of wild mulberry silkworm, *B. mandarina*, were collected from Tokyo University of Agriculture and Technology in Fuchu (35° 41' N) and the Gunma Sericultural Technology Center at Maebashi (36° 24' N). The oviposited non-diapause eggs were incubated at 25DD and 15DD. Larvae were reared on mulberry leaves at 25–27 °C under 16L8D, 8L16D, and 24L0D. Pupae used in the experiments were collected within 12 h after each ecdysis. Pupae were incubated at 25 °C to allow for adult development.

The percentage of diapause eggs was estimated by counting the number of eggs in diapause and those not in diapause in each egg batch after the non-diapause eggs hatched. The results are expressed as the average percentage of diapause in each egg batch^{8,9}. For *B. mandarina*, the eggs were counted using a SZ61 stereo microscope (Olympus, Tokyo, Japan). Pupal-adult development lasted 12–26 d in these experiments, and a few pupae did not eclose within one month, as described in a previous report³². The unclosed pupae were not used for calculation of the diapause eggs inducing activity.

Thionin staining and immunostaining. Thionin staining was performed as previously described⁸. The eggs were fixed in Carnoy's fixative for 1 d at 4 °C. The fixed eggs were treated with a gradient concentration of ethanol for 10 min. Following 5 min of boiling, the chorion was dissected, and the eggs were transferred into a thionine solution (0.07% thionine and 0.3% phenol dissolved in 80% ethanol) for 2 h. The stained eggs were rinsed with 80% ethanol four times and dehydrated with a gradient concentration of ethanol for 10 min after each rinse. The eggs were then soaked in benzene to make the yolk transparent. The embryos were observed using an M165 FC stereomicroscope (Leica, Wetzlar, Germany).

The immunoreaction procedures were adapted as previously reported¹¹. The brain–SG complex or the CC and CA complex were dissected in fixative containing 4% paraformaldehyde, 7% picric acid, 10 mM MgCl₂, 5 mM EGTA–NaOH, and 0.5 M HEPES–NaOH (pH 6.9) and incubated at 4 °C overnight. The fixed tissues were stored in 90% methanol containing 50 mM EGTA at –20 °C until use. The fixed and stored tissues were hydrated through decreasing concentrations of methanol and washed with PBS containing 0.2% Tween-20 (PBT). Tissue samples were soaked in PBS containing 2% Tween-20 for two nights, washed with PBT, blocked with PBT containing 5% heat-inactivated goat serum (Wako, Osaka, Japan) and 2% BSA, and incubated with anti-DH[N]¹¹ at 1:2500 at 4 °C overnight. The signal was detected with a Cy3-labeled IgG (Jackson ImmunoResearch Lab, West Grove, PA, USA) diluted to 1:1500 using an FV1000-D confocal microscope (Olympus).

Injection of picrotoxin (PTX) and peptides. PTX was purchased from Sigma Aldrich (St. Louis, MI, USA). The chemical synthetic Crz peptide was purchased from Abbotec (Escondido, CA, USA). DH was

obtained from Operon Biotechnologies (Tokyo, Japan). PTX and peptides were dissolved in distilled water and peanut oil, respectively, and 10- μ L solutions of various doses were injected into pupae a day after pupation through the intersegmental membrane between the second and third abdominal segments.

cDNA cloning. Eggs were collected the day before hatching. Ovaries were dissected from pupae a day after pupation. Total RNA was extracted from eggs and ovaries using TRI-reagent (Molecular Research Center, Inc., Cincinnati, OH, USA) and then subjected to first-strand DNA synthesis using ReverTra Ace qPCR RT Master Mix with gDNA Remover (Toyobo, Osaka, Japan). By searching the highly-homologous sequences of each *DHR* and *TRPA1* cDNA for *B. mandarina* in the genomic database SilkBase (<http://silkbase.ab.a.u-tokyo.ac.jp/cgi-bin/index.cgi>), we designed the primers (Supplementary Table S1) to amplify each open reading frame sequence using RT-PCR.

Electrophysiological assay. TRPA1 channel property was characterized by expressing the channel in *Xenopus laevis* oocytes, and ionic currents were measured by a two-electrode voltage clamp method as previously described^{33,34}. In brief, *BmoTRPA1*, *BmaTRPA1a*, and *BmaTRPA1b* were cloned into a pOX plasmid vector, and complementary RNA (cRNA) was synthesized with the mMACHINE SP6 kit (Thermo Fisher Scientific, Waltham, MA, USA) using a linearized pOX vector containing TRPA1 as a template. Fifty nanoliters of each TRPA1 cRNA (50 or 100 ng/ μ L) was then injected into defolliculated *Xenopus* oocytes, and ionic currents were observed 2–6 d post-injection. Oocytes were voltage-clamped at –60 mV, and ionic currents were recorded using an OC-725C amplifier (Warner Instruments, Holliston, MA, USA) with a 1-kHz low-pass filter and digitized at 5 kHz using a Digidata 1440 Digitizer (Molecular Devices, San Jose, CA, USA). For thermal stimulation, heated or chilled ND96 bath solutions containing (mM) 96 NaCl, 2 KCl, 1.8 CaCl₂, 1 MgCl₂, and 5 HEPES (pH 7.6), were applied by perfusion. The temperature was monitored with a thermistor located just beside the oocytes using a TC-344B controller (Warner Instruments). Heat-evoked currents for TRPA1 were obtained from *Xenopus* oocytes from two independent preparations, and apparent thermal activation thresholds for TRPA1 were determined with an Arrhenius plot that was generated using Clampfit 10.4 (Molecular Devices) and Origin 9 J (OriginLab, Northampton, MA, USA).

TALEN construction and screening of KO silkworm. The TALEN-based mutant lines were constructed according to the previous reports^{8,35}. Briefly, TALEN targets were searched using TAL Effector Nuclease Targeter 2.0 (<https://tale-nt.cac.cornell.edu>) in the coding regions of target genes. DNA constructs containing TAL segments were prepared using a Golden Gate TALEN kit (Addgene, Cambridge, MA, USA). TALEN mRNAs were then synthesized using the mMACHINE T7 Ultra kit (Ambion, Carlsbad, CA, USA). The mRNA of each TALEN was mixed at a concentration of 0.5 μ g/ μ L for microinjection. Non-diapause eggs of the Kosetsu strain were collected within 1 h after oviposition during the syncytial blastoderm stage. The TALEN mRNA mixture was injected into the eggs using a glass needle (uMPm-02; Daiwa Union, Iida, Japan) attached to a manipulator (kaikopuchu-STDU1; Daiwa Union) and FemtoJet (Eppendorf, Hamburg, Germany).

For screening germline mutagenesis, G₀ adults were mated with *wt*. The oviposited G₁ eggs were collected, and approximately ten eggs from each brood were pooled for genomic DNA extraction using DNAzol reagent (Thermo Fisher Scientific). The DNA fragment containing the targeted region of interest was amplified by PCR using Takara Ex Taq (Takara, Tokyo, Japan) and specific primers (Supplementary Table S1). To test for mutagenesis, the PCR product of *BmoTRPA1* was treated with the Surveyor Mutation Detection kit (IDT, Tokyo, Japan). The mutated PCR products were checked by sequencing. The broods containing mutated sequences were reared, and mutated G₁ adults were crossed with the siblings carrying the same mutation. Homozygous mutants were obtained after confirmation by sequencing of the target region in the G₂ or G₃ egg genome.

DH extraction and titer measurement. DH was extracted from the hemolymph as previously described⁸. DH extraction was performed at ZT6 (ZT = zeitgeber time, ZT = 0 corresponds to light on). DH levels were measured using a time-resolved fluoroimmunoassay as described previously⁸.

Statistical analysis. Statistical parameters, including definitions and exact values of *n*, are provided in the relevant figures or corresponding figure legends. Statistical analyses were performed in Microsoft Excel 2011 with the software add-in Toukei-Kaiseki Ver. 3.0 (Esumi, Tokyo, Japan). The significance of differences in diapause egg-inducing activity was evaluated using the Steel–Dwass test. Other data were compared using Student's *t*-tests. Data are expressed as the mean \pm SD. *P* < 0.05 was considered significant; ns, non-significant; *, *P* < 0.05; **, *P* < 0.01; ***, *P* < 0.001.

Data availability

The datasets in the current study are available from the corresponding author on reasonable request.

Received: 30 January 2021; Accepted: 31 March 2021

Published online: 13 April 2021

References

- Nakagaki, M., Takei, R., Nagashima, E. & Yaginuma, T. Cell-cycles in embryos of the silkworm, *Bombyx-mori* - G2-arrest at diapause stage. *Roux Arch. Dev. Biol.* **200**, 223–229 (1991).
- Yamashita, O. & Hasegawa, K. in *Comprehensive Insect Physiology, Biochemistry and Pharmacology* Vol. 1 (eds G.A. Kerkut & L.I. Gilbert) 407–434 (Pergamon Press, 1985).

3. Kogure, M. The influence of light and temperature on certain characters of the silkworm, *Bombyx mori*. *J. Dep. Agric. Kyushu Univ.* **4**, 1–93 (1933).
4. Watanabe, K. Studies on the voltinism of the silkworm, *Bombyx mori*. *Bull. Sericult. Exp. Sta. (Tokyo)* **6**, 411–455 (1924).
5. Denlinger, D. L., Yocum, G. D. & Rinehart, J. P. in *Insect Endocrinology* (ed L.I. Gilbert) 430–463 (Academic Press, 2012).
6. Shimizu, I. & Hasegawa, K. Photoperiodic induction of diapause in the silkworm, *Bombyx mori*: location of the photoreceptor using a chemiluminescent paint. *Physiol. Entomol.* **13**, 81–88 (1988).
7. Tsuchida, K. & Yoshitake, N. Effect of different artificial diets on diapause induction under controlled temperature and photoperiod in the silkworm, *Bombyx mori* L. *Physiol. Entomol.* **8**, 333–338 (1983).
8. Shiomi, K. *et al.* Disruption of diapause induction by TALEN-based gene mutagenesis in relation to a unique neuropeptide signaling pathway in *Bombyx*. *Sci. Rep.* **5**, 15566 (2015).
9. Tsuchiya, R. *et al.* Maternal GABAergic and GnRH/corazonin pathway modulates egg diapause phenotype of the silkworm *Bombyx mori*. *Proc. Natl. Acad. Sci. U. S. A.* **118**, e2020028118 (2021).
10. Sato, Y. *et al.* Precursor polyprotein for multiple neuropeptides secreted from the subesophageal ganglion of the silkworm *Bombyx mori* - characterization of the cDNA-encoding the diapause hormone precursor and identification of additional peptides. *Proc. Natl. Acad. Sci. U. S. A.* **90**, 3251–3255 (1993).
11. Hagino, A., Kitagawa, N., Imai, K., Yamashita, O. & Shiomi, K. Immunoreactive intensity of FXPRL amide neuropeptides in response to environmental conditions in the silkworm, *Bombyx mori*. *Cell Tissue Res.* **342**, 459–469 (2010).
12. Yamashita, O., Imai, K., Saito, H., Shiomi, K. & Sato, Y. Phe-X-Pro-Arg-Leu-NH(2) peptide producing cells in the central nervous system of the silkworm, *Bombyx mori*. *J. Insect. Physiol.* **44**, 333–342 (1998).
13. Homma, T. *et al.* G protein-coupled receptor for diapause hormone, an inducer of *Bombyx* embryonic diapause. *Biochem. Biophys. Res. Commun.* **344**, 386–393 (2006).
14. Sato, A. *et al.* Embryonic thermosensitive TRPA1 determines transgenerational diapause phenotype of the silkworm, *Bombyx mori*. *Proc. Natl. Acad. Sci. U. S. A.* **111**, E1249–1255 (2014).
15. Goldsmith, M. R., Shimada, T. & Abe, H. The genetics and genomics of the silkworm, *Bombyx mori*. *Annu. Rev. Entomol.* **50**, 71–100 (2005).
16. Sasaki, C. On the affinity of our wild and domestic silkworms. *Annot. Zool. Jap.* **2**, 33–41 (1898).
17. Yoshitake, N. Phylogenetic aspects on the origin of Japanese race of the silkworm, *Bombyx mori* L. *J. Seric. Sci. Jpn.* **37**, 83–87 (1968).
18. Yukuhiro, K., Sezutsu, H., Itoh, M., Shimizu, K. & Banno, Y. Significant levels of sequence divergence and gene rearrangements have occurred between the mitochondrial Genomes of the wild mulberry silkworm, *Bombyx mandarina*, and its close relative, the domesticated silkworm, *Bombyx mori*. *Mol. Biol. Evol.* **19**, 1385–1389 (2002).
19. Miyata, T. A generic revision of the Japanese Bombycidae, with description of a new genus (Lepidoptera). *Tinea* **8**, 190–199 (1970).
20. Murakami, A. & Imai, H. T. Cytological evidence for holocentric chromosomes of the silkworms, *Bombyx mori* and *B. mandarina*, (Bombycidae, Lepidoptera). *Chromosoma* **47**, 167–178 (1974).
21. Yokoyama, T. Reproduction and natural enemies of the wild mulberry silkworm (*Bombyx mandarina*). *Sanshi-Konchu Biotec* **88**, 25–38 (2019).
22. Xia, Q. Y. *et al.* Complete resequencing of 40 genomes reveals domestication events and genes in silkworm (*Bombyx*). *Science* **326**, 433–436 (2009).
23. Umeya, Y. Embryonic hibernation and diapause in insects from the viewpoint of the hibernating-eggs of the silkworm. *Bull. Sericult. Exp. Sta.* **12**, 393–480 (1946).
24. Yamashita, O. & Yaginuma, T. in *Insects at Low Temperature* (eds Jr. R. E. Lee & D. L. Denlinger) 424–445 (Chapman and Hall, 1991).
25. Komoto, N. & Tomita, S. Distribution and seasonal occurrence of the wild mulberry silkworm (*Bombyx mandarina*) in Japan. *Sanshi-Konchu Biotec* **88**, 7–23 (2019).
26. Ohmura, S. Research on the behavior and ecological characteristics of the wild silkworm, *Bombyx mandarina*. *Bull. Seric. Exp. Sta. Jpn.* **13**, 79–130 (1950).
27. Kobayashi, J. Effects of photoperiod on the induction of egg diapause of tropical races of the domestic silkworm, *Bombyx-Mori*, and the wild silkworm, *Bombyx-mandarina*. *JARQ Jpn. Agric. Res. Q.* **23**, 202–205 (1990).
28. Xu, W. H., Sato, Y. & Yamashita, O. Molecular characterization of the cDNA encoding diapause hormone and pheromone biosynthesis activating neuropeptide in *Bombyx mandarina*. *J. Seric. Sci. Jpn.* **68**, 373–379 (1999).
29. Li, T. B. *et al.* Diverse sensitivities of TRPA1 from different mosquito species to thermal and chemical stimuli. *Sci. Rep.* <https://doi.org/10.1038/s41598-019-56639-w> (2019).
30. Zhong, L. X. *et al.* Thermosensory and nonthermosensory isoforms of *Drosophila melanogaster* TRPA1 reveal heat-sensor domains of a thermoTRP channel. *Cell Rep.* **1**, 43–55 (2012).
31. Denlinger, D. L., Hahn, D. A., Merlin, C., Holzapfel, C. M. & Bradshaw, W. E. Keeping time without a spine: what can the insect clock teach us about seasonal adaptation?. *Philos. Trans. R. Soc. Lond. B* <https://doi.org/10.1098/rstb.2016.0257> (2017).
32. Kobayashi, J. Effects of photoperiod on the duration of pupal stage of the wild silkworm, *Bombyx mandarina* Moore. *Wild Silkworms '89-'90*, 57–64 (1991).
33. Saito, S. *et al.* Heat and noxious chemical sensor, chicken TRPA1, as a target of bird repellents and identification of its structural determinants by multispecies functional comparison. *Mol. Biol. Evol.* **31**, 708–722 (2014).
34. Saito, S., Saito, C. T., Nozawa, M. & Tominaga, M. Elucidating the functional evolution of heat sensors among *Xenopus* species adapted to different thermal niches by ancestral sequence reconstruction. *Mol. Ecol.* **28**, 3561–3571 (2019).
35. Takasu, Y., Tamura, T., Sajwan, S., Kobayashi, I. & Zurovec, M. The use of TALENs for nonhomologous end joining mutagenesis in silkworm and fruitfly. *Methods* **69**, 46–57 (2014).

Acknowledgments

This research was funded by Grants-in-Aid from the Ministry of Education, Science, Sports, and Culture of Japan. We are also indebted to the Division of Gene Research, Research Center for Human and Environmental Sciences for providing facilities for these studies.

Author contributions

K.S. designed the research. Y.K., S.S., M.S., M.K., Y.T., H.S., Y.K., M.T., A.K., and K.S. performed the research. Y.K., S.S., and K.S. analyzed the data. T.Y., S.S., and K.S. drafted the manuscript with support from all authors.

Competing interests

The authors declare no competing interests.

Additional information

Supplementary Information The online version contains supplementary material available at <https://doi.org/10.1038/s41598-021-87590-4>.

Correspondence and requests for materials should be addressed to K.S.

Reprints and permissions information is available at www.nature.com/reprints.

Publisher's note Springer Nature remains neutral with regard to jurisdictional claims in published maps and institutional affiliations.



Open Access This article is licensed under a Creative Commons Attribution 4.0 International License, which permits use, sharing, adaptation, distribution and reproduction in any medium or format, as long as you give appropriate credit to the original author(s) and the source, provide a link to the Creative Commons licence, and indicate if changes were made. The images or other third party material in this article are included in the article's Creative Commons licence, unless indicated otherwise in a credit line to the material. If material is not included in the article's Creative Commons licence and your intended use is not permitted by statutory regulation or exceeds the permitted use, you will need to obtain permission directly from the copyright holder. To view a copy of this licence, visit <http://creativecommons.org/licenses/by/4.0/>.

© The Author(s) 2021